In colony allorecognition assays, three of four isogenic pairs receiving control morpholinos fused within 24 hours of ampullae contact. By contrast, no reactions were observed in isogenic pairs receiving BHF translation-blocking morpholinos (n = 6), despite constant physical contact over observational periods ranging from 2 to 7 days (Fig. 3D, fig. S19, and table S8). To exclude nonspecific effects, we also tested *BHF* splice-inhibiting morpholinos, using the progeny of wild-type colonies (*15*). Within 2 days of ampullae contact, all control pairs had fused (n = 2) or rejected (n = 1), whereas colony pairs receiving splice-inhibiting morpholinos did not react (n = 5) (figs. S20 and S21, table S9, and movies S1 and S2). These data support our genomic analysis and indicate that BHF participates in fusion and rejection initiation.

In the jawed vertebrates, the MHC is a haplotype, each sublocus of which specifies a different recognition process, usually by unique subsets of cells (*18*–*20*). By contrast, the *B. schlosseri* Fu/HC locus is a single gene (*BHF*) embedded in a haplotype of several genes with high polymorphism. Unlike the secreted (*sFuHC*) and membrane-bound (*mFuHC*) genes, *BHF* has none of the domains expected for a cell surface–recognition protein or, in fact, domains that are conserved throughout protein evolution. Because *BHF* does not follow biological precedence by either sequence or domains, future investigations of this gene will likely reveal new mechanisms of recognition.

The ability to reliably predict histocompatibility outcomes on the basis of a single gene has broad implications for the study of allorecognition. For example, after vasculature fusion, stem cells from each *B. schlosseri* colony compete to overtake germline and/or somatic lineages (*21*–*24*). Stem cell competition may lead to elimination of the other colony's genome or may produce a chimeric colony with mixed genotypes. To date, induction of chimerism using hematopoietic stem-cell transplantation is the only way to achieve long-term donor-specific tolerance to human organ allografts (*25*). Chimerism can be short-lived, and if lost, the threat of allograft rejection emerges. *B. schlosseri* is a unique species for studying stem cell–mediated chimerism, and such research will be facilitated by BHF.

References and Notes

1. A. Nakashima, T. Shima, K. Inada, M. Ito, S. Saito, *Am. J. Reprod. Immunol.* **67**, 304 (2012).
2. G. Girardi, Z. Prohászka, R. Bulla, F. Tedesco, S. Scherjon, *Mol. Immunol.* **48**, 1621 (2011).
3. M. Colonna, S. Jonjic, C. Watzl, *Nat. Immunol.* **12**, 107 (2011).
4. D. F. LaRosa, A. H. Rahman, L. A. Turka, *J. Immunol.* **178**, 7503 (2007).
5. F. Delsuc, H. Brinkmann, D. Chourrout, H. Philippe, *Nature* **439**, 965 (2006).
6. H. Oka, H. Watanabe, *Proc. Jpn. Acad.* **33**, 657 (1957).
7. H. Oka, H. Watanabe, *Bull. Mar. Biol. Stat. Asamushi.* **10**, 153 (1960).
8. A. Sabbadin, *Rend. Accad. Naz. Lincei. Ser.* **32**, 1031 (1962).
9. V. L. Scofield, J. M. Schlumpberger, L. A. West, I. L. Weissman, *Nature* **295**, 499 (1982).
10. A. W. De Tomaso, Y. Saito, K. J. Ishizuka, K. J. Palmeri, I. L. Weissman, *Genetics* **149**, 277 (1998).
11. A. W. De Tomaso, I. L. Weissman, *Immunogenetics* **55**, 480 (2003).
12. A. W. De Tomaso *et al.*, *Nature* **438**, 454 (2005).
13. A. Voskoboynik *et al.*, *eLife* **2**, e00569 (2013).
14. I. Letunic, T. Doerks, P. Bork, SMART 7: recent updates to the protein domain annotation resource. *Nucleic Acids Res.* **40**, D302 and (2012).
15. Materials and methods are available as supplementary materials on *Science* Online.
16. B. Rinkevich, J. Douek, C. Rabinowitz, G. Paz, *Dev. Comp. Immunol.* **36**, 718 (2012).
17. M. Oren, J. Douek, Z. Fishelson, B. Rinkevich, *Dev. Comp. Immunol.* **31**, 889 (2007).
18. The MHC sequencing consortium, *Nature* **401**, 921 (1999).
19. M. Hirano, S. Das, P. Guo, M. D. Cooper, *Adv. Immunol.* **109**, 125 (2011).
20. L. J. Dishaw, G. W. Litman, *Curr. Biol.* **19**, R286 (2009).
21. D. S. Stoner, I. L. Weissman, *Proc. Natl. Acad. Sci. U.S.A.* **93**, 15254 (1996).
22. D. S. Stoner, B. Rinkevich, I. L. Weissman, *Proc. Natl. Acad. Sci. U.S.A.* **96**, 9148 (1999).
23. D. J. Laird, A. W. De Tomaso, I. L. Weissman, *Cell* **123**, 1351 (2005).
24. A. Voskoboynik *et al.*, *Cell Stem Cell* **3**, 456 (2008).
25. D. H. Sachs, M. Sykes, T. Kawai, A. B. Cosimi, *Semin. Immunol.* **23**, 165 (2011).

Acknowledgments: We thank B. Rinkevich for pointing out the difficulty with the original cFuHC assignments and T. Snyder, J. Okamoto, L. Me, L. Ooi, A. Dominguez, C. Lowe, K. Uhlinger, L. Crowder, S. Karten, C. Patton, L. Jerabek, and T. Storm for invaluable technical advice and help. A. De Tomaso provided the fosmid sequence used to characterize *cFuHC* (*12*) (table S5). D.P., A.V., and S.R.Q. have filed U.S. and international patent applications (61/532,882 and 13/608,778, respectively) entitled "Methods for obtaining a sequence." This invention allows for the sequencing of long continuous (kilobase scale) nucleic acid fragments using conventional short read–sequencing technologies, useful for consensus sequencing and haplotype determination. This study was supported by NIH grants 1R56AI089968, R01GM100315, and 1R01AG037968 awarded to I.L.W., A.V., and S.R.Q., respectively, and the Virginia and D. K. Ludwig Fund for Cancer Research awarded to I.L.W. D.S. was supported by NIH grant K99CA151673-01A1 and Department of Defense Grant W81XWH-10-1-0500, and A.M.N., D.M.C., D.S., and I.K.D. were supported by a grant from the Siebel Stem Cell Institute and the Thomas and Stacey Siebel Foundation. The data in this paper are tabulated in the main manuscript and in the supplementary materials. BHF, sFuHC, and mFuHC sequences are available in GenBank under accession numbers KF017887-KF017889, and the RNA-Seq data are available on the Sequence Read Archive (SRA) database: BioProject SRP022042.

Supplementary Materials

www.sciencemag.org/cgi/content/full/341/6144/384/DC1
Materials and Methods
Figs. S1 to S21
Tables S1 to S9
References (*26*–*42*)
Movies S1 and S2

19 March 2013; accepted 30 May 2013
10.1126/science.1238036

Creating a False Memory in the Hippocampus

Steve Ramirez,[1]* Xu Liu,[1,2]* Pei-Ann Lin,[1] Junghyup Suh,[1] Michele Pignatelli,[1] Roger L. Redondo,[1,2] Tomás J. Ryan,[1,2] Susumu Tonegawa[1,2]†

Memories can be unreliable. We created a false memory in mice by optogenetically manipulating memory engram–bearing cells in the hippocampus. Dentate gyrus (DG) or CA1 neurons activated by exposure to a particular context were labeled with channelrhodopsin-2. These neurons were later optically reactivated during fear conditioning in a different context. The DG experimental group showed increased freezing in the original context, in which a foot shock was never delivered. The recall of this false memory was context-specific, activated similar downstream regions engaged during natural fear memory recall, and was also capable of driving an active fear response. Our data demonstrate that it is possible to generate an internally represented and behaviorally expressed fear memory via artificial means.

Neuroscience aims to explain how brain activity drives cognition. Doing so requires identification of the brain regions that are specifically involved in producing internal mental representations and perturbing their activity to see how various cognitive processes are affected. More specifically, humans have a rich repertoire of mental representations generated internally by processes such as conscious or unconscious recall, dreaming, and imagination (*1*, *2*). However, whether these internal representations can be combined with external stimuli to generate new memories has not been vigorously studied.

Damage to the hippocampus impairs episodic memory (*3*–*8*). Recently, using fear conditioning in mice as a model of episodic memory, we identified a small subpopulation of granule cells in the dentate gyrus (DG) of the hippocampus as contextual memory-engram cells. Optogenetic stimulation of these cells is sufficient to activate behavioral recall of a context-dependent fear memory formed by a delivery of foot shocks. This finding provided an opportunity to investigate how the internal representation of a specific context can be associated with external stimuli of high valence. In particular, a hypothesis of great interest is

[1]RIKEN–Massachusetts Institute of Technology (MIT) Center for Neural Circuit Genetics at the Picower Institute for Learning and Memory, Department of Biology and Department of Brain and Cognitive Sciences, MIT, Cambridge, MA 02139, USA. [2]Howard Hughes Medical Institute, MIT, Cambridge, MA 02139, USA.

*These authors contributed equally to this work.
†Corresponding author. E-mail: tonegawa@mit.edu

whether artificially activating a previously formed contextual memory engram while simultaneously delivering foot shocks can result in the creation of a false fear memory for the context in which foot shocks were never delivered. To address this, we investigated whether a light-activated contextual memory in the DG or CA1 can serve as a functional conditioned stimulus (CS) in fear conditioning.

Our system uses c-fos-tTA transgenic mice, in which the promoter of the *c-fos* gene drives the expression of the tetracycline transactivator (tTA) to induce expression of a gene of interest downstream of the tetracycline-responsive element (TRE) (*8*–*12*). We injected an adeno-associated virus (AAV) encoding TRE-ChR2-mCherry into the DG or CA1 of c-fos-tTA animals (Fig. 1A). Channelrhodopsin-2 (ChR2)–mCherry expression was completely absent in the DG of animals that had been raised with doxycycline (Dox) in the diet (on Dox) (Fig. 1B). Exploration of a novel context under the condition of Dox withdrawal (off Dox) elicited an increase in ChR2-mCherry expression (Fig. 1C). We confirmed the functionality of the expressed ChR2-mCherry by recording light-induced spikes in cells expressing ChR2-mCherry from both acute hippocampal slices and in anaesthetized animals (Fig. 1, D to F). Furthermore, optical stimulation of ChR2-mCherry–expressing DG cells induced cFos expression throughout the anterior-posterior axis of the DG (fig. S1, A to I).

We first took virus-infected and fiber-implanted animals off Dox to open a time window for labeling cells activated by the exploration of a novel context (context A) with ChR2-mCherry. The animals were then put back on Dox to prevent any further labeling. The next day, we fear-conditioned this group in a distinct context (context B) while optically reactivating the cells labeled in context A. On the following 2 days, we tested the animals' fear memory in either the original context A or a novel context C (Fig. 1G). If the light-reactivated cells labeled in context A can produce a functional CS during fear conditioning in context B, then the animals should express a false fear memory by freezing in context A, but not in context C.

First, we examined the degree of overlap of the cell populations activated in contexts A and C (*8*, *11*). We injected a group of c-fos-tTA mice with an AAV virus encoding TRE-ChR2-mCherry and exposed them to context A while off Dox so as to label activated DG cells with ChR2-mCherry. These animals were then immediately placed back on Dox to prevent further labeling. The next day, half of the animals were exposed to context C, and the other half were reexposed to context A as a control. Both groups were euthanized 1.5 hours later. DG cells activated by the first exposure to context A were identified by ChR2-mCherry expression, and cells activated by the exposure to context C or the reexposure to context A were identified by the expression of endogenous c-Fos. The c-Fos generated by the first exposure to context A had been degraded by the time the animals underwent their second context exposure (*11*). Contexts A and C recruited statistically independent populations of DG cells. In contrast, two exposures to context A recruited substantially overlapping cell populations in the dorsal DG (Fig. 2, A to E).

When DG cells activated by the exposure to context A were reactivated with light during fear conditioning in a distinct context B, the animals subsequently froze in context A at levels significantly higher than the background levels, whereas freezing in context C did not differ from background levels (Fig. 2F). This increased freezing in context A was not due to generalization, because a control group expressing only mCherry that underwent the exact same training protocol did not show the same effect (Fig. 2F). A separate group of animals expressing ChR2–enhanced yellow fluorescent protein

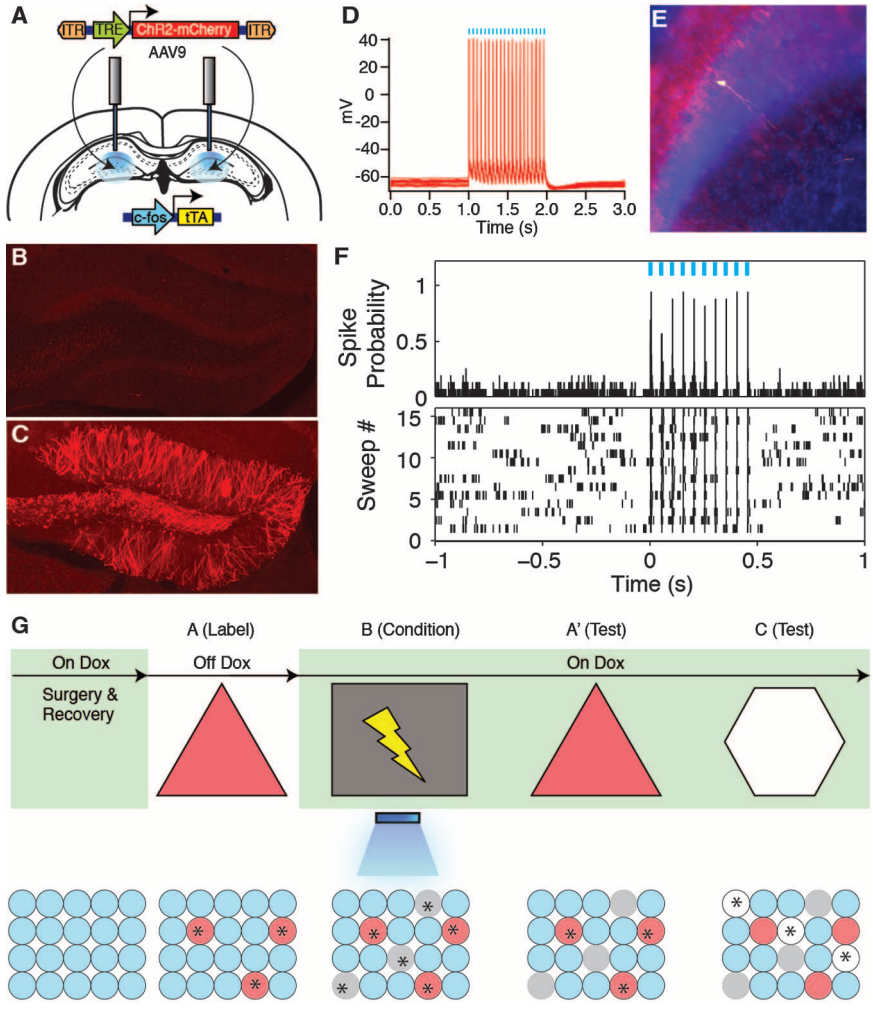

Fig. 1. Activity-dependent labeling and light-activation of hippocampal neurons, and the basic experimental scheme. (**A**) The c-fos-tTA mice were bilaterally injected with AAV_9-TRE-ChR2-mCherry and implanted with optical fibers targeting DG. (**B**) While on Dox, exploration of a novel context did not induce expression of ChR2-mCherry. (**C**) While off Dox, exploration of a novel context induced expression of ChR2-mCherry in DG. (**D**) Light pulses induced spikes in a CA1 neuron expressing ChR2-mCherry. The recorded neuron is shown labeled with biocytin in (**E**). (**F**) Light pulses induced spikes in DG neurons recorded from a head-fixed anesthetized c-fos-tTA animal expressing ChR2-mCherry. (**G**) Basic experimental scheme. Post-surgery mice were taken off Dox and allowed to explore context A in order to let DG or CA1 cells become labeled with ChR2-mCherry. Mice were put back on Dox and fear conditioned in context B with simultaneous delivery of light pulses. Freezing levels were then measured in both the original context A and a novel context C. The light green shading indicates the presence of Dox in the diet during corresponding stages of the scheme. Prime indicates the second exposure to a given context. The yellow lightning symbol and blue shower symbol indicate foot shocks and blue light delivery, respectively. Red circles represent neurons encoding context A that are thus labeled with ChR2-mCherry. Gray and white circles represent neurons encoding context B and C, respectively. Asterisks indicate neurons activated either by exposure to context or light stimulation.

(EYFP) instead of ChR2-mCherry in the DG that underwent the same behavioral schedule also showed increased freezing in context A (fig. S2A).

New experimental and control groups of mice were taken off Dox in context A in order to label activated cells and then placed in context C on the following day while back on Dox. In this experiment, although conditioning took place after the formation of both context A and context C memories, only those cells encoding context A were reactivated by light during fear conditioning. Subsequently, all groups of mice displayed background levels of freezing in context C. In contrast, in the context A test the next day, the experimental group showed increased freezing levels as compared with those of the mCherry-only group, confirming that the recall of the false memory is specific to context A (Fig. 2G). This freezing was not observed in another ChR2-mCherry group that underwent the same behavioral protocol but without light stimulation during fear conditioning in context B, or in a group in which an immediate shock protocol was administered in context B with light stimulation of context A cells (Fig. 2G and fig. S3). In a separate group of animals, we labeled cells active in context C rather than context A and repeated similar experiments as above. These animals showed freezing in context C but not context A (fig. S2B).

The hippocampus processes mnemonic information by altering the combined activity of subsets of cells within defined subregions in response to discrete episodes (*11*–*13*). Therefore, we investigated whether applying the same parameters and manipulations to CA1 as we did to the DG could form a false memory. We first confirmed that light could activate cells expressing ChR2-mCherry along the anterior-posterior axis of the CA1 similar to the DG (fig. S1, J to R). Also similar to the DG (Fig. 2, A to E), the overlap of active CA1 cells was significantly lower across contexts (A and C) as compared with that of a reexposure to the same context (A and A). However, the degree of overlap for the two contexts was much greater in CA1 (30%) than in the DG (~1%). When we labeled CA1 cells activated in context A and reactivated these cells with light during fear conditioning in context B, no increase in freezing was observed in the experimental group expressing ChR2-mCherry as compared with the mCherry-only control group in either context A or context C, regardless of whether the animals were exposed to context C or not before fear conditioning in context B (Fig. 2, M and N).

The simultaneous availability of two CSs can sometimes result in competitive conditioning; the memory for each individual CS is acquired less strongly as compared with when it is presented alone, and the presentation of two simultaneous CSs to animals trained with a single CS can also lead to decrement in recall (*14*). In our experiments, it is possible that the light-activated DG cells encoding context A interfered with the acquisition or expression of the genuine fear memory for context B. Indeed, upon reexposure to context B, the experimental group froze significantly less than the group that did not receive light during fear conditioning or the group expressing mCherry alone (Fig. 3A and fig. S4). During light-on epochs in the context B test, freezing increased in the experimental group and decreased in the group that did not receive light during fear conditioning (Fig. 3A and fig. S2C). We conducted similar experiments with mice in which the manipulation was targeted to the CA1 region and found no differences in the experimental or control groups during either light-off or light-on epochs of the context B test (fig. S5A).

Memory recall can be induced for a genuine fear memory by light reactivation of the corresponding engram in the DG (*8*). To investigate

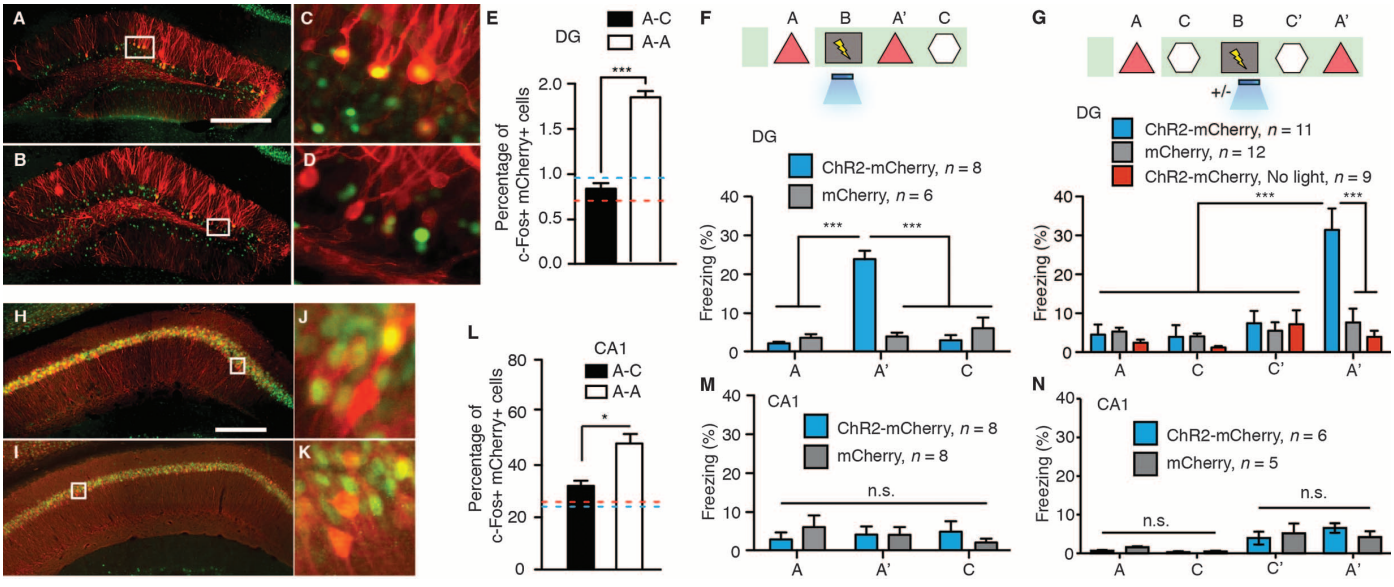

Fig. 2. Creation of a false contextual fear memory. (**A** to **E**) c-fos-tTA mice injected with AAV_9-TRE-ChR2-mCherry in the DG were taken off Dox and exposed to context A in order to label the activated cells with mCherry (red), then put back on Dox and exposed to the same context A [(A) and (C)] or a novel context C [(B) and (D)] 24 hours later so as to let activated cells express c-Fos (green). Images of the DG from these animals are shown in (A) to (D), and the quantifications are shown in (E) (n = 4 subjects each; ***P < 0.001, unpaired Student's t test). Blue and red dashed lines indicate the chance level of overlap for A-A and A-C groups, respectively. (**F**) (Top) Training and testing scheme of animals injected with AAV_9-TRE-ChR2-mCherry or AAV_9-TRE-mCherry. Various symbols are as explained in Fig. 1. (Bottom) Animals' freezing levels in context A before fear conditioning and in context A and C after fear conditioning [n = 8 subjects for ChR2-mCherry group, and n = 6 subjects for mCherry group; ***P < 0.001, two-way analysis of variance (ANOVA) with repeated measures followed by Bonferroni post-hoc test]. (**G**) (Top) Training and testing scheme of animals injected with AAV_9-TRE-ChR2-mCherry or AAV_9-TRE-mCherry. One control group injected with AAV_9-TRE-ChR2-mCherry did not receive light stimulation during fear conditioning (ChR2-mCherry, no light). (Bottom) Animals' freezing levels in context A and C before and after fear conditioning (n = 11 subjects for ChR2-mCherry group, n = 12 subjects for mCherry, and n = 9 subjects for ChR2-mCherry, no-light groups; ***P < 0.001, two-way ANOVA with repeated measures followed by Bonferroni post-hoc test). (**H** to **L**) Animals underwent the same protocol as in (A) to (E), except the virus injection was targeted to CA1. Representative images of CA1 from these animals are shown in (H) to (K), and the quantifications are shown in (L) (n = 4 subjects each; *P = 0.009, unpaired Student's t test). (**M**) Same as (F), except the viral injection and implants were targeted to CA1 (n = 8 subjects for ChR2-mCherry and mCherry groups; n.s., not significant; two-way ANOVA with repeated measures followed by Bonferroni post-hoc test). (**N**) Same as (G), except the viral injection and implants were targeted to CA1 (n = 6 subjects for ChR2-mCherry group and n = 5 subjects for mCherry group). Scale bar in (A) and (H), 250 μm.

whether this applies to a false fear memory, we examined fear-memory recall of experimental and control groups of mice in a distinct context (context D) with light-off and light-on epochs (Fig. 3B). All groups exhibited background levels of freezing during light-off epochs. The experimental group, however, froze at significantly higher levels (~25%) during light-on epochs. This light-induced freezing in context D was not observed in control animals that underwent the same behavioral schedule but did not receive light during fear conditioning in context B, in animals expressing mCherry alone, in animals receiving immediate shock, or in animals in which CA1 was manipulated instead (Fig. 3B and figs. S2D, S3C, S4C, and S5B).

Moreover, we quantified the levels of c-Fos expression in the basolateral amygdala (BLA) and the central amygdala (CeA) during the recall of a false and genuine fear memory (*15*–*20*). Both sessions elicited a significant increase in c-Fos–positive cells in the BLA and CeA compared with a control group exploring a neutral context (Fig. 3, C to F).

Last, a new cohort of mice was trained in a conditioned place avoidance (CPA) paradigm (*21*). Naïve animals did not show an innate preference for either chamber across multiple days (fig. S6A). An experimental group injected with the ChR2-mCherry virus and a control group injected with the mCherry-only virus were taken off Dox and exposed to one chamber of the CPA apparatus in order to label the DG cells activated in this chamber. These animals were then placed back on Dox and on the following day were exposed to the opposite chamber. Next, the mice were fear conditioned in a different context with light stimulation. The following day, they were placed back into the CPA apparatus, and their preference between the chambers was measured (Fig. 4A). After conditioning, the experimental group showed a strong preference for the unlabeled chamber over the labeled chamber, whereas the mCherry-only group spent an equal amount of time exploring both chambers (Fig. 4, B to D, and fig. S6B). Exposure to the two chambers activated a statistically independent population of DG cells (Fig. 4, E to K). We conducted similar behavioral tests targeting the CA1 subregion of the hippocampus, and the experimental group did not show any chamber preference (Fig. 4, L and M).

Our results show that cells activated previously in the hippocampal DG region can subsequently serve as a functional CS in a fear-conditioning paradigm when artificially reactivated during the delivery of a unconditioned stimulus (US). The consequence is the formation of a false associative fear memory to the CS that was not naturally available at the time of the US delivery. This is consistent with previous findings that high-frequency stimulation of the perforant path, an input to DG, can serve as a CS in a conditioned suppression paradigm (*22*).

Memory is constructive in nature; the act of recalling a memory renders it labile and highly

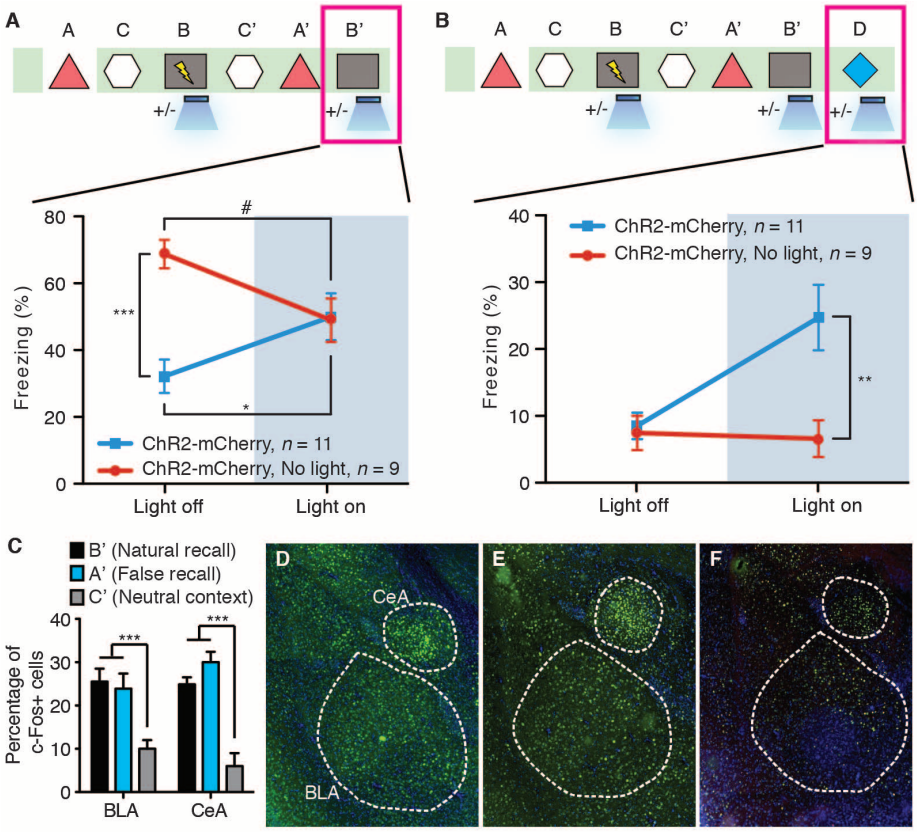

Fig. 3. The false and genuine fear memories interact with each other, and both recruit the amygdala. (**A**) Animals that underwent the behavioral protocol shown in Fig. 2G were reexposed to context B, and the freezing levels were examined both in the absence and presence of light stimulation (n = 11 subjects for ChR2-mCherry group and n = 9 subjects for ChR2-mCherry, no-light group; *P = 0.027; ***P < 0.001; #P = 0.034, two-way ANOVA with repeated measures followed by Bonferroni post-hoc test). (**B**) Animals that underwent the behavioral protocol shown in (A) were placed in a novel context D, and the freezing levels were examined both in the absence and presence of light stimulation (n = 11 subjects for ChR2-mCherry group and n = 9 subjects for ChR2-mCherry, no-light group; **P = 0.007, two-way ANOVA with repeated measures followed by Bonferroni post-hoc test). (**C**) Three groups of mice underwent the training shown in (A) and were euthanized after testing in either context B (natural recall), A (false recall), or C (neutral context). The percentage of c-Fos–positive cells was calculated for each group in basolateral amygdala (BLA) and central amygdala (CeA) (n = 6 subjects each; ***P < 0.001). (**D** to **F**) Images for natural recall, false recall, or neutral context.

susceptible to modification (*23*, *24*). In humans, memory distortions and illusions occur frequently. These phenomena often result from the incorporation of misinformation into memory from external sources (*25*–*27*). Cognitive studies in humans have reported robust activity in the hippocampus during the recall of both false and genuine memories (*28*). However, human studies performed using behavioral and functional magnetic resonance imaging techniques have not been able to delineate the hippocampal subregions and circuits that are responsible for the generated false memories. Our experiments provide an animal model in which false and genuine memories can be investigated at the memory-engram level (*29*). We propose that optical reactivation of cells that were naturally activated during the formation of a contextual memory induced the retrieval of that memory, and the retrieved memory became associated with an event of high valence (a foot shock) to form a new but false memory. Thus, the experimental group of animals showed increased freezing in a context in which they were never shocked (context A). Although our design for the formation and expression of a false memory was for a laboratory setting, and the retrieval of the contextual memory during conditioning occurred by artificial means (light), we speculate that the formation of at least some false memories in humans may occur in natural settings through the internally driven retrieval of a previously formed memory and its association with concurrent external stimuli of high valence.

Our experiments also allowed us to examine the dynamic interaction between the false and genuine memories at different stages of the memory process. During the acquisition phase, the artificial contextual information (context A by light activation) either competed with the genuine contextual cues (context B by natural exposure) for the valence of the US (foot shock), or may have interfered with the perception of the genuine

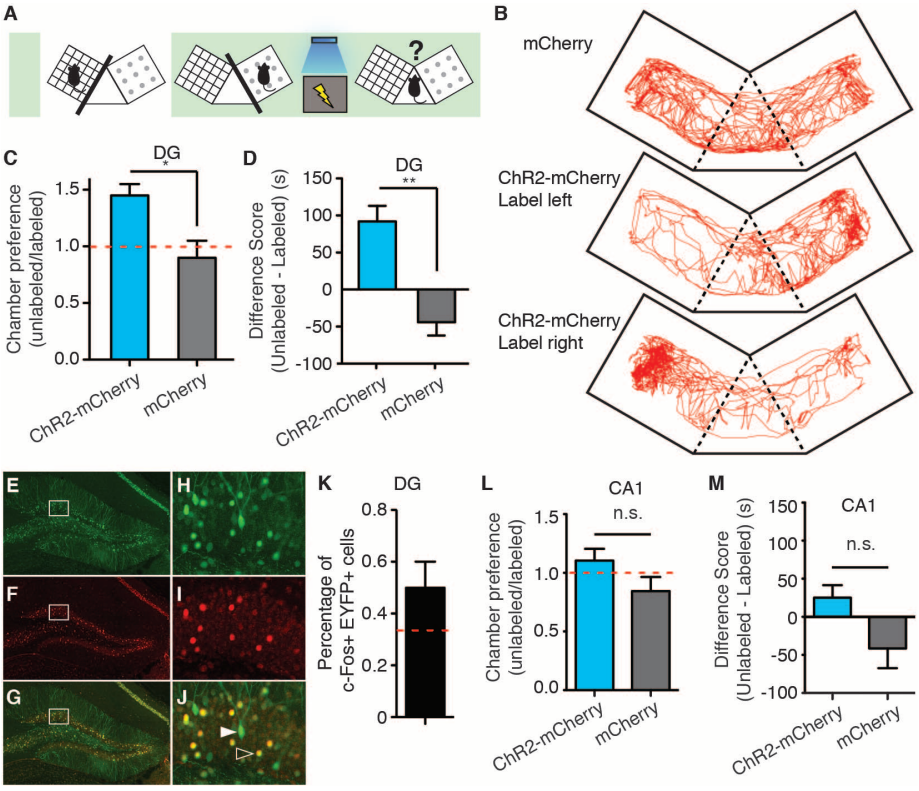

Fig. 4. The false memory supports active fear behavior. (**A**) The scheme for conditioned place-avoidance paradigm. Various symbols are as explained in Fig. 1. (**B**) Locomotion traces during testing from animals injected with AAV_9-TRE-mCherry (top), or animals injected with AAV_9-TRE-ChR2-mCherry and DG cells subsequently labeled, corresponding to either the left (middle) or right (bottom) chamber. (**C** and **D**) ChR2-mCherry and mCherry group preferences for the labeled versus unlabeled chambers as shown by the ratio (C) or the difference in duration of the time spent in each chamber (D). ($n = 8$ subjects; $^*P = 0.013$; $^{**}P = 0.008$, unpaired Student's t test). The red dashed line indicates no preference. (**E** to **K**), c-fos-tTA mice injected with AAV_9-TRE-EYFP in the DG were taken off Dox and exposed to one chamber in order to label the activated cells with EYFP (green) then put back on Dox and exposed to the opposite chamber 24 hours later to let activated cells express c-Fos (red). Expression of EYFP [(E) and (H)], expression of c-Fos [(F) and (I)], and a merged view [(G) and (J)] are shown. Solid arrows indicate cells expressing EYFP. Open arrows indicate cells expressing c-Fos. These cells appear yellow because they express both endogenous c-Fos (red) and the nuclear-localized c-fos-shEGFP (green) from the mouse line (*10*). Quantifications from the dorsal blades of the DG are shown in (K) ($n = 4$ subjects). Red dashed lines indicate the chance level of overlap. (**L** and **M**) Same as (C) and (D), except the viral injection and implants were targeted to CA1 ($n = 6$ subjects each group).

contextual cues. This resulted in reduced expression of both false and genuine fear memories compared with the strength of recall attainable after normal fear conditioning (Fig. 3A, the two groups during the light-off epoch). This could also be related to the overshadowing effects for multiple CSs (*30*). During the recall phase in context B, the false memory and the genuine memory were either additive (Fig. 3A, the with-light group during light-off and light-on epochs) or competitive (Fig. 3A, the no light group during light-off and light-on epochs). All of these observations are consistent with the predictions of an updated Rescorla-Wagner componential model for two independent CSs and suggest that the light-activated artificial CS is qualitatively similar to the genuine CS (*14*).

A previous study applied a similar experimental protocol with pharmacosynthetic methods and failed to see increased freezing upon reexposure to either context A or context B. Instead, they observed a synthetic memory that could only be retrieved by the combination of both contexts A and B (*9*). A key difference in their system is that the c-Fos–expressing cells in the entire forebrain were labeled and reactivated over an extended period by a synthetic ligand. We propose that activating neurons in much wider spatial and temporal domains may favor the formation of a synthetic memory, which may not be easily retrievable by the cues associated with each individual memory. In contrast, activating neurons in a more spatially (only small populations of DG cells) and temporally restricted manner (only a few minutes during light stimulation) may favor the formation of two distinct (false and genuine) memories as observed in our case. In line with this hypothesis, when we manipulated CA1 cells by the same procedures as the ones used for DG cells, we could not create a false memory (freezing in context A). In CA1, the overlap of the cell populations activated by consecutive exposures to a pair of contexts is much greater than in the DG. Although additional work is needed to reveal the nature of CA1 engrams, we hypothesize that our negative CA1 behavioral data could be a result of contextual engrams relying less on a population code and increasingly on a temporal code as they travel through the trisynaptic circuit (*4*, *11*–*13*).

References and Notes

1. D. L. Schacter, D. R. Addis, R. L. Buckner, *Nat. Rev. Neurosci.* **8**, 657–661 (2007).
2. E. Pastalkova, V. Itskov, A. Amarasingham, G. Buzsáki, *Science* **321**, 1322–1327 (2008).
3. H. Gelbard-Sagiv, R. Mukamel, M. Harel, R. Malach, I. Fried, *Science* **322**, 96–101 (2008).
4. C. J. MacDonald, K. Q. Lepage, U. T. Eden, H. Eichenbaum, *Neuron* **71**, 737–749 (2011).
5. G. Buzsáki, E. I. Moser, *Nat. Neurosci.* **16**, 130–138 (2013).
6. T. J. McHugh *et al.*, *Science* **317**, 94–99 (2007).
7. D. Tse *et al.*, *Science* **316**, 76–82 (2007).
8. X. Liu *et al.*, *Nature* **484**, 381–385 (2012).
9. A. R. Garner *et al.*, *Science* **335**, 1513–1516 (2012).
10. L. G. Reijmers, B. L. Perkins, N. Matsuo, M. Mayford, *Science* **317**, 1230–1233 (2007).
11. S. Kubik, T. Miyashita, J. F. Guzowski, *Learn. Mem.* **14**, 758–770 (2007).
12. J. F. Guzowski, B. L. McNaughton, C. A. Barnes, P. F. Worley, *Nat. Neurosci.* **2**, 1120–1124 (1999).
13. J. K. Leutgeb, S. Leutgeb, M. B. Moser, E. I. Moser, *Science* **315**, 961–966 (2007).
14. S. E. Brandon, E. H. Vogel, A. R. Wagner, *Behav. Brain Res.* **110**, 67–72 (2000).
15. J. H. Han *et al.*, *Science* **323**, 1492–1496 (2009).
16. M. T. Rogan, U. V. Stäubli, J. E. LeDoux, *Nature* **390**, 604–607 (1997).
17. J. P. Johansen *et al.*, *Proc. Natl. Acad. Sci. U.S.A.* **107**, 12692–12697 (2010).
18. S. Maren, G. J. Quirk, *Nat. Rev. Neurosci.* **5**, 844–852 (2004).
19. H. Li *et al.*, *Nat. Neurosci.* **16**, 332–339 (2013).
20. S. Ciocchi *et al.*, *Nature* **468**, 277–282 (2010).
21. S. Lammel *et al.*, *Nature* **491**, 212–217 (2012).
22. V. Doyère, S. Laroche, *Hippocampus* **2**, 39–48 (1992).
23. K. Nader, G. E. Schafe, J. E. Le Doux, *Nature* **406**, 722–726 (2000).
24. F. C. Bartlett, *Remembering: A Study in Experimental and Social Psychology* (Cambridge Univ. Press, Cambridge, 1932).
25. E. F. Loftus, *Nat. Rev. Neurosci.* **4**, 231–234 (2003).
26. D. L. Schacter, E. F. Loftus, *Nat. Neurosci.* **16**, 119–123 (2013).
27. H. L. Roediger, K. B. McDermott, *J. Exp. Psychol. Learn. Mem. Cogn.* **24**, 803–814 (1995).
28. R. Cabeza, S. M. Rao, A. D. Wagner, A. R. Mayer, D. L. Schacter, *Proc. Natl. Acad. Sci. U.S.A.* **98**, 4805–4810 (2001).
29. S. M. McTighe, R. A. Cowell, B. D. Winters, T. J. Bussey, L. M. Saksida, *Science* **330**, 1408–1410 (2010).
30. I. P. Pavlov, *Conditioned Reflexes* (Oxford University Press, Oxford, 1927).

Acknowledgments: We thank S. Huang, M. Serock, A. Mockett, J. Zhou, and D. S. Roy for help with the experiments; J. Z. Young and K. L. Mulroy for comments and discussions on the manuscript; and all the members of the Tonegawa lab for their support. This work was supported by the RIKEN Brain Science Institute.

Supplementary Materials

www.sciencemag.org/cgi/content/full/341/6144/387/DC1
Materials and Methods
Figs. S1 to S6
References

12 April 2013; accepted 2 July 2013
10.1126/science.1239073